


Cite this: *RSC Adv.*, 2024, 14, 6146

# One pot application of a green chemistry-based finish for cotton fabric, providing hydrophobic, flame retardant, and antimicrobial properties

Rabia Sharif,<sup>a</sup> \*a Haji Ghulam Qutab,<sup>a</sup> Khalid Mahmood,<sup>a</sup> Saba Gul,<sup>a</sup> Naveed Ramzan,<sup>b</sup> Muhammad Mohsin,<sup>c</sup> Ahtesham Wahlah,<sup>d</sup> Rizwan Nasir,<sup>e</sup> Palwasha Fazal<sup>a</sup> and Barkat Ali<sup>a</sup>

Fluorinated and formaldehyde-based compounds impart excellent hydrophobicity and flame-retardant properties to cotton fabrics. However, they come with various health and environmental risks. A novel hydrophobic, flame retardant, and antimicrobial finishing agent free from fluorine and formaldehyde was synthesized. The diammonium phosphate octadecyl citrate (DAPOC) was synthesized by using stearic acid (octadecanoic acid), citric acid (propane-1,2,3-tricarboxylic acid), and diammonium hydrogen phosphate. It was grafted onto the cotton fabrics by employing the conventional pad-dry-cure method. The results indicated that this newly developed finish could be chemically bonded to cotton fabrics through C–O–C covalent bonds. The contact angle of the cotton fabric finished with a 12% concentration of the finishing agent reached 151.9°. Additionally, the finished cotton fabrics displayed evident flame-retardant properties. After undergoing 20 laundering cycles, DAPOC maintained strong hydrophobic and flame-retardant characteristics, demonstrating its durability. The chemical structure of DAPOC was verified by nuclear magnetic resonance spectroscopy (<sup>1</sup>H-NMR). The thermogravimetric analysis confirmed the flame-retardant nature of the treated cotton fabric samples. Scanning electron microscopy (SEM), Energy dispersive X-ray analysis (EDX), and Fourier-transform infrared spectroscopy (FTIR) results demonstrated the successful grafting of the newly created finish onto the cotton fiber. X-ray diffraction (XRD) spectra depicted that the crystalline structure of finished cotton fabric remained mostly unaltered. Furthermore, the finished cotton fabric exhibited commendable antimicrobial properties due to the inclusion of citric acid.

Received 19th November 2023  
Accepted 14th February 2024

DOI: 10.1039/d3ra07931g

rsc.li/rsc-advances

## Introduction

The textile sector is diverse and vast as it produces commodities with innovative applications in daily life. The worldwide competing products of the textile industry include fiber, fabric, raw materials, home furnishing, and most importantly apparel.<sup>1,2</sup> Technical textiles are manufactured with their non-aesthetic role as the major concerns.<sup>3,4</sup> The basic idea behind the functional protective textiles such as hydrophobic,<sup>5,6</sup> antimicrobial,<sup>7,8</sup> crease and soil resistant,<sup>8,9</sup> and flame retardant<sup>10,11</sup> is to provide comfort and protection to end users. Cotton fabric

is biodegradable, versatile, and used in various applications. The apparel and home decor industry<sup>12,13</sup> widely use cotton fabric due to its attractive properties such as breathability, comfortable, economical, soft, and warm.<sup>14,15</sup>

Nonetheless, natural cellulose, despite being biogenetic, possesses flammability,<sup>16,17</sup> making it susceptible to fire accidents that can result in significant human and economic losses. Conversely, cotton harbors have abundant hydroxyl groups and pores,<sup>16</sup> providing an optimal environment for water absorption and bacterial growth and rendering it susceptible to staining. Consequently, in everyday settings or environments such as hospitals, laboratories, or places demanding high antibacterial standards, cotton fabrics must exhibit flame-retardant, self-cleaning, and antimicrobial attributes.<sup>18,19</sup> Waterproof and flame-retardant coated fabrics find extensive use in both civilian and military sectors,<sup>20–22</sup> including applications like outdoor attire, automotive interiors, firefighter, tents, and military uniforms.<sup>23</sup> Among the numerous methods for super-hydrophobic and flame-resistance treatment of fabric, modification in surface properties emerges as the most efficient and user-friendly approach.<sup>24,25</sup>

<sup>a</sup>Department of Chemical, Polymer and Process Engineering, University of Engineering and Technology, Faisalabad Campus, Lahore, Faisalabad, Pakistan. E-mail: rabia.sharif@uet.edu.pk

<sup>b</sup>Department of Chemical Engineering, University of Engineering and Technology Lahore, Pakistan

<sup>c</sup>Department of Textile Engineering, University of Engineering and Technology Lahore, Faisalabad Campus, Faisalabad, Pakistan

<sup>d</sup>Rescue Emergency 1122, Faisalabad, Pakistan

<sup>e</sup>Department of Chemical Engineering, University of Jeddah, Asfan Road, Jeddah, Saudi Arabia



In recent times, nanocellulose has emerged as a highly intriguing environmentally friendly material suitable as an additive in polymers. This is mainly attributed to its ability to improve the mechanical characteristics of the resultant nanocomposites. Maturi *et al.* conducted the synthesis of a range of nanocomposites designed for vat photopolymerization. The nanocomposites were formulated using commercial resin and cellulose nanocrystals, both of which underwent modification with fatty acids sourced from safflower oil. This alteration enabled the hydrophobization of cellulose nanocrystals (CNCs), ensuring their effective dispersal within the polymeric resin.<sup>26</sup> In another study, the modification process involves the adsorption of quaternary ammonium salts, drawing inspiration from the techniques used to modify layered silicates in an organic manner. The modified series of cellulose nanocrystals (CNCs) obtained from this process can be dried from solvent and exhibit the potential for forming well-dispersed nanocomposites when combined with non-polar polymers.<sup>27</sup>

Surfaces with a sliding angle of less than 10° degrees and a water contact angle larger than 150° have shown signs of being extremely hydrophobic and non-wetting.<sup>28</sup> The hydrophobic properties of a surface are contingent upon its structural roughness and chemical composition. Hence, a hydrophobic surface of cotton fabric is typically generated *via* a two-step process: (1) generating rough formations on the cotton base using a nanoscale material and (2) applying chemical modifications to the substrate with materials possessing low surface energy. Fluorinated compounds find extensive application in crafting hydrophobic surfaces owing to their diminished surface energy.<sup>29,30</sup>

Nonetheless, fluorine can carry the potential to pose harm to both humans and the environment.<sup>31</sup> Furthermore, they have been identified as carcinogenic,<sup>32</sup> capable of damaging the immune systems of children,<sup>33</sup> and associated with reduced female fertility.<sup>34</sup> Consequently, numerous countries have prohibited the use of fluorinated compounds in creating hydrophobic surfaces.<sup>8,35,36</sup> Utilizing a blend of nanoscale and microparticles alongside low surface energy materials is a method for crafting superhydrophobic surfaces. However, applying this technique to cotton fabrics by coating can decrease the durability of treated samples.<sup>37</sup> This occurs due to the inability of the coated material to form covalent bonds with the cellulose fibers.<sup>38</sup> In a specific study, the achievement of hydrophobic cotton was realized by surface modifying cellulose with triglycerides derived from rapeseed oil, soybean oil, coconut oil and olive oil.<sup>39</sup>

The literature has documented the application of diverse bio-based repellents, such as octadecanoic acid (stearic acid)<sup>8</sup> and hexadecanoic acid (palmitic acid).<sup>36</sup> Recent research has uncovered the potential of self-repairing attributes in hydrophobic surfaces to enhance their durability.<sup>40</sup> Adding cross-linkers to the basic formulation can increase the durability of short-chain or nondurable water and oil-repelling agents.<sup>41,42</sup>

The significant issue with cotton fabrics is their pronounced flammability. Indeed, flame-retardant properties in cotton fabrics are commonly attained by applying flame-retardant finishes.<sup>43,44</sup> Flame retardants are typically categorized into

four groups: halogen-based, organophosphorus-based, inorganic metallic oxide, and nitrogen-based flame retardants.<sup>45,46</sup> Halogen-based flame retardants have been prohibited because of their toxicity.<sup>12</sup> Cotton fabrics rendered flame-resistant through the application of phosphorus-based flame retardants, such as Pyrovatex CP and Proban, may release formaldehyde during use.<sup>47</sup>

In recent times, there have been reports of bio-derived flame retardants like DNA (Deoxyribonucleic acid) and phytic acid.<sup>48</sup> Additionally, novel nanomaterials such as graphene,<sup>49</sup> nano silicon dioxide<sup>50</sup>, and carbon nanotubes<sup>51</sup> have been employed as flame retardants. While these methods are simple and convenient, the resulting flame-retardant cotton fabrics often lack durability. While numerous methods exist to confer flame resistancy or water repellency to cotton fabrics, achieving both functions simultaneously is a rarity. Nevertheless, various industries demand cotton fabrics that possess both flame-resistance and superhydrophobic properties.

Thirumalaisamy Suryaprabha and colleagues achieved flame-retardant properties and superhydrophobic in cotton fabrics using silver, copper, and bismuthiol I. The finished fabric exhibited exceptional superhydrophobicity and good resistance to rubbing, albeit they displayed poor durability after washing.<sup>52</sup> In a separate study,<sup>53</sup> researchers employed self-assembly and *in situ* sol-gel technology to create flame-retardant and hydrophobic cotton fabrics. However, these did not meet the washing durability requirements for practical applications. Another group of researchers developed a sol-gel reaction method to produce superhydrophobic and flame-resistance finish on cotton fabric.<sup>54</sup> Researchers should explore innovative phosphorus-based reactive flame retardants that do not contain formaldehyde to produce durable flame-retardant cotton fabrics.

Until now, the coated cotton fabrics had superhydrophobic characteristics and demonstrated impressive flame retardancy. However, the discussion did not delve into the durability of the treated cotton fabric. It's important to emphasize that coatings with low surface energy and flame-resistant properties have yet to be covalently bonded to cellulose. In this research, a fluorine-free bio-based long-chain fatty known as stearic acid and a phosphorus-based formaldehyde-free diammonium hydrogen phosphate (DAHP) reacted with bio-based crosslinker citric acid in one pot. The newly developed recipe diammonium phosphate octadecyl citrate (DAPOC) was employed on the pristine cotton *via* the conventional pad-dry-cure method to gain hydrophobicity and flame retardancy.

## Materials and methods

Fabric composed primarily of bleached cotton was used in this investigation. The fabric weighed 142 grams per square meter and had a simple weave pattern measuring 1 × 1 (GSM). Sigma Aldrich was the supplier of the water-repellent stearic acid (SA), flame-retardant diammonium hydrogen phosphate (DAHP), cross-linker citric acid (CA), catalyst sodium hypophosphite (SHP), enhancer triethanolamine (TEA), and solvent isopropyl alcohol (IPA).



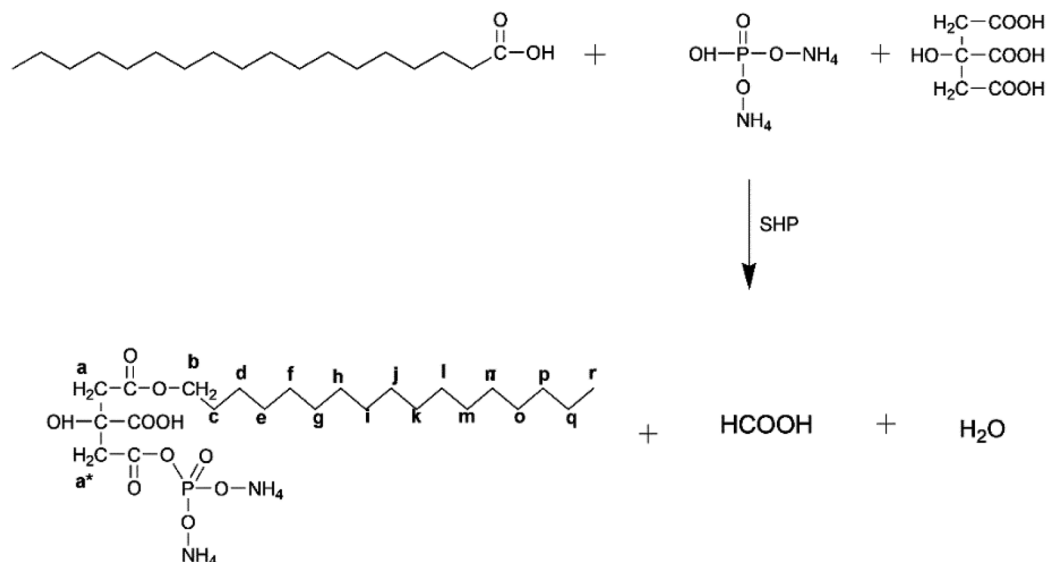


Fig. 1 Synthesis of diammonium phosphate octadecyl citrate (DAPOC).

In a stirred vacuum reactor, the following components were introduced: stearic acid (12 grams), diammonium hydrogen phosphate (7 grams), citric acid (5 grams), sodium hypophosphite monohydrate (SHP) (5 grams), and tri-ethanolamine (TEA) (5 grams) as an enhancer. The esterification reaction took place at a temperature of 160 °C and was carried out for 3 hours. The resulting synthetic DAPOC was subsequently diluted with a mixture of isopropyl alcohol and water, both in equal proportions to the synthetic finish. Fig. 1 illustrates the scheme of chemical reactions that took place.

The formulated finish was administered to the cotton fabric using three distinct mass concentrations: 4%, 8%, and 12%. The conventional Pad-Dry-Cure method (Color smith, UK) with 70% pick up was used to apply the coating. Following the padding process, the fabric underwent a 3 minutes drying process at 100 °C and a 2 minutes curing process at 180 °C using a HY0120A model stenter machine, as shown in Fig. 2. All specimens underwent conditioning at 20 °C with a relative humidity of  $65 \pm 2\%$  for a minimum of 4 hours prior to any testing. The washing durability was assessed using the AATCC 61-2006 standard test. Contact angle of both coated and uncoated fabrics was assessed by the drop shape analysis system DSA30. Moreover, the antimicrobial activity of the fabric against *Escherichia coli* and *Staphylococcus aureus* bacteria was assessed following the AATCC 147 test method. The chemical structure of DAPOC was acquired by H-NMR spectroscopy (Magritek Spinsolve Bench Top), at 600 MHz NMR spectrometer using Advance Neo Technology and TXI probe. The surface topography of both treated and untreated cotton fabric was scrutinized using a Scanning Electron Microscope (SEM). The morphological analysis used the SEM AIS 1800C model at 10 kV. Prior to testing, all samples underwent gold coating for four minutes.

To identify the functional groups in the synthesized recipe, Fourier-transform infrared (FTIR) spectroscopy was employed, utilizing the Agilent CARY 630 apparatus. The scan range

spanned from 4000 to 50  $\text{cm}^{-1}$ , with a resolution of 4  $\text{cm}^{-1}$ . Energy Dispersive X-ray Spectroscopy (EDX) with a 5 keV beam energy was employed for elemental analysis of the cotton fabric. Thermogravimetric Analysis (TGA) of the samples was conducted to document the mass loss during heating from 25 °C to 600 °C, employing a heating rate of 10 °C  $\text{min}^{-1}$ . The analysis was carried out using a NETZSCH TG 209F1 Libra evolution analyzer. The XRD (X-ray Diffraction) diffractogram of the cotton samples was recorded using X'Pert Pro diffractometer (Netherland) with Cu K $\alpha$  radiation ( $\lambda = 0.1540 \text{ nm}$ ) and a generator was running at 45 kV and 40 mA. Char length was determined through the vertical burning test (BS 5438:1989, Test 2B). The limiting oxygen index (LOI) was measured in accordance with ASTM D2863, utilizing the YZS-100A LOI apparatus. Additionally, the smoldering cigarette test was performed following the EN 1021:1994 standard.

## Results and discussions

### H-NMR spectroscopy

The chemical structure of diammonium phosphate octadecyl citrate (DAPOC) is elucidated by  $^1\text{H}$ -NMR ( $\text{CDCl}_3$ , 600 MHz) as shown in Fig. 3. The peak (r) at 0.89 ppm represents hydrogen atom in  $\text{CH}_3$  (Methyl at terminal). The peak (d-q) at 1.25–1.28 ppm corresponds to a large number of hydrogen atoms in a long chain of  $\text{CH}_2$  from  $\text{C}_4$ – $\text{C}_{17}$ . The peak (c) at 1.68 ppm corresponds to hydrogen atom in  $\text{CH}_2$  of  $\text{C}_3$ . The peak (b) at 2.3 ppm represents the  $\text{CH}_2$  at  $\alpha$  position to  $\text{O}=\text{C}-\text{O}$ . The peaks (a) at 3.85 ppm depict the  $\text{CH}_2$  at  $\beta$  position to  $\text{O}=\text{C}-\text{O}$ .<sup>55</sup> The peak (a\*) at 4.45 ppm is showing  $\text{CH}_2$  bonded to  $\text{O}=\text{C}-\text{O}$  adjacent to phosphorus.

### Hydrophobic behavior

The wetting behavior of cotton fabrics is shown in Fig. 4(a)–(e). It is observed upon application of water (liquid) droplets to the



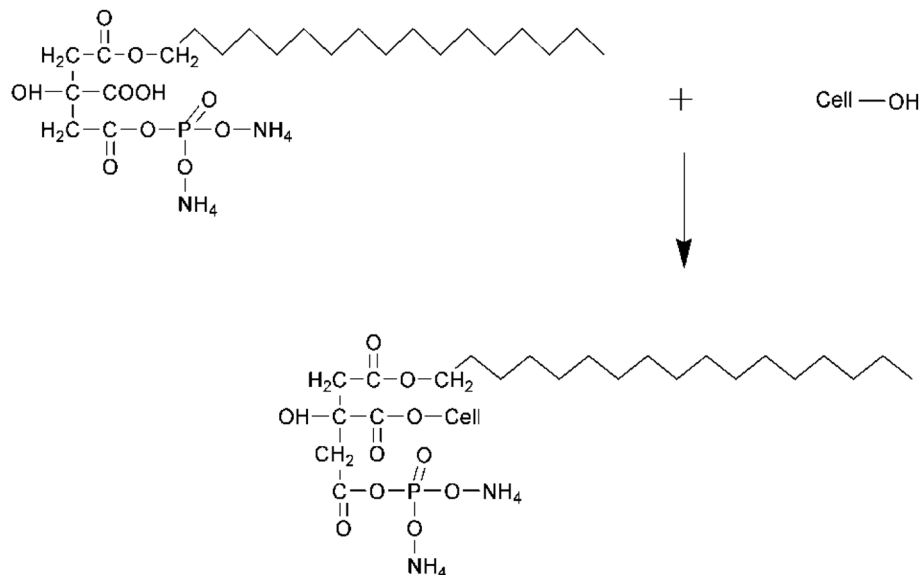
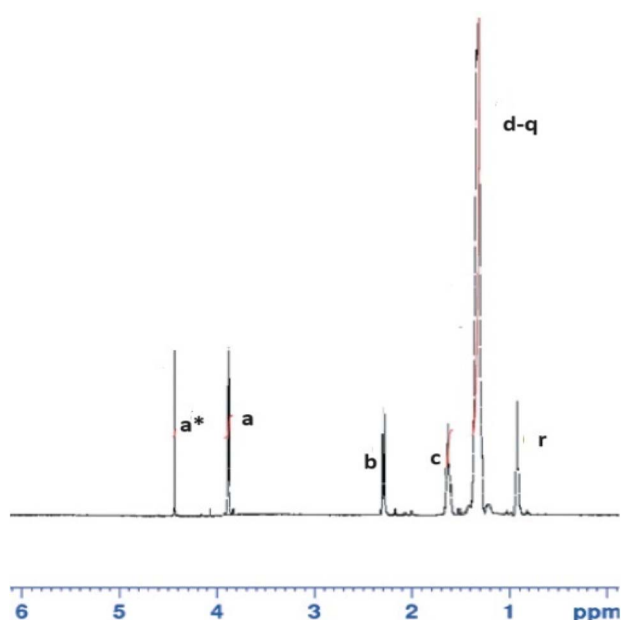


Fig. 2 Grafting of DAPOC on cellulose.

Fig. 3  $^1\text{H}$ -NMR spectra of DAPOC.

surface of untreated cotton, the fabric quickly became wet. This is attributed to hydrophilic characteristics of the hydroxyl groups present in cotton fabric, resulting in a contact angle of  $0^\circ$ . In contrast, finished cotton fabrics evinced remarkable hydrophobic properties. Cotton fabric treated with mass concentrations of 4%, 8% and 12% showed water contact angles (WCAs) of  $147^\circ$ ,  $149.2^\circ$ , and  $151.9^\circ$ , respectively as shown in Fig. 3. Notably, the WCAs for samples treated with 8% finishing agent approximately approach the benchmark for super hydrophobicity, set at  $150^\circ$ .<sup>56</sup> However, cotton fabric treated with 12% of the finishing agents exhibits a water contact angle slightly higher than the benchmark.

With increased concentration of the finishing agent, a progressive rise in the contact angles was observed on the coated cotton fabric. These findings affirm that the hydrophobic finishing agent effectively bestows remarkable hydrophobic properties upon cotton fabrics, as shown in Fig. 4(e).

### Vertical flammability test

A vertical burner test was conducted on both pristine fabric and cotton fabric coated with varying mass concentrations (4%, 8%, and 12%) of the finishing agent to assess their fire-resistant qualities. The control sample exhibited an after-flame duration of 10 seconds and an after-glow duration of 25 seconds. It underwent an intense burning, leaving only a small char residue (refer to Fig. 5(a)). In Fig. 5(b)–(d), it can be noted that the char lengths for cotton fabric treated with finishing agents of 4%, 8%, and 12% were 85 mm, 67 mm, and 48 mm, respectively. None of the treated samples experienced ignition. These outcomes indicate that the finished cotton fabrics displayed outstanding flame-retardant properties.

The control sample displayed an LOI of 18.0%. Be contrary to, the cotton fabrics treated with 4%, 8%, and 12% finished fabric exhibited higher LOI values of 24.0%, 25.5%, and 27.0%, respectively. Notably, all treated cotton fabrics demonstrated elevated LOI values compared to the control. Even after undergoing 20 wash cycles, these values remained elevated at 23.2%, 24.6%, and 26.4%, surpassing the standard LOI value for cotton fabric.<sup>57</sup> These findings confirm that the DAPOC effectively imparts flame retardancy and durability to cotton fabric.

The cotton fabrics that underwent treatment demonstrated increased resistance to smoldering after being extinguished. In comparison, the untreated cotton fabric experienced intense burning; however, the flame on the treated fabric was notably gentler. This was due to incorporating the phosphorous base flame-retardant in the recently formulated recipe, which formed a chemical covalent bond with the cotton fabrics. Following 20



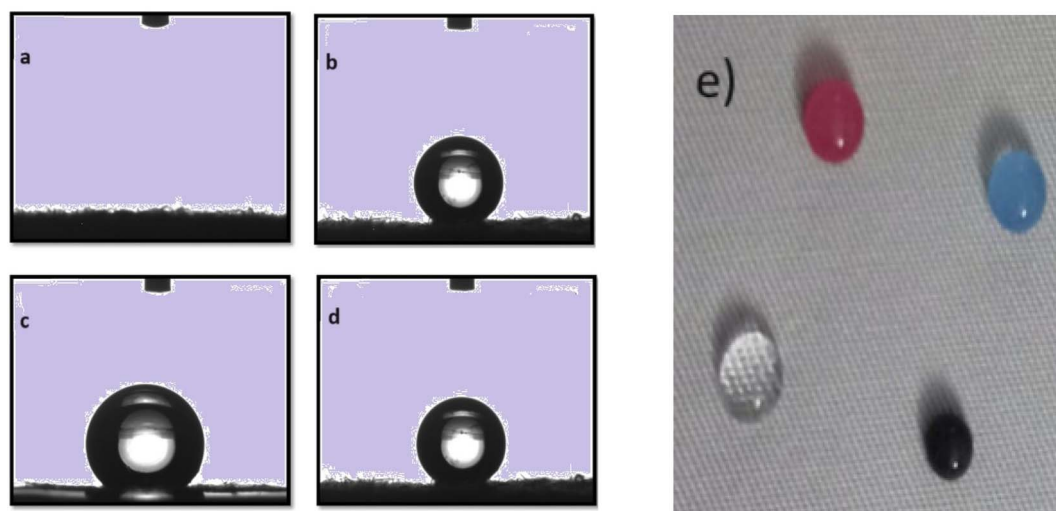


Fig. 4 (a) Water droplet on a pristine fabric, (b)–(d) water contact angle of cotton fabric treated with 4%, 8%, and 12% mass concentrations of DAPOC (e) water and ink droplet on treated cotton fabric.

wash cycles, the treated cotton fabric reduced its flame resistance, as assessed by the smoldering cigarette test, as shown in Table 1.

#### Spectroscopy analysis using Fourier-transform infrared

The FTIR spectrum reveals a discernible contrast in absorption bands between the pristine and treated fabrics, signifying the emergence of a novel band in the treated samples. This affirms

that the newly introduced finish has led to a shift in the wavelength of the functional groups. This indicates a notable alteration in the chemical composition and bonding configurations, suggesting potential changes in the fabric's properties and performance.

The peaks in absorption observed between 3500–3000 and 3000–2800  $\text{cm}^{-1}$  were attributed to the stretching of primary alcohol group in cellulose-OH and anti-symmetric stretching of C-H bonds,<sup>58</sup> respectively. The intense peaks observed at 2914 and

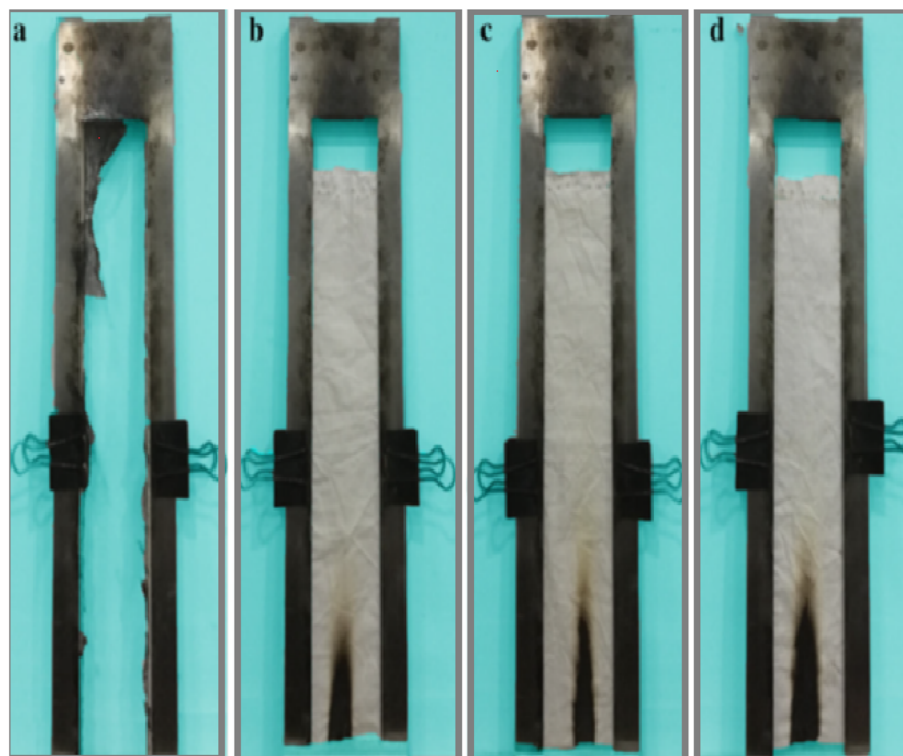


Fig. 5 The vertical flammability burning test (a) pristine sample and (b)–(d) samples finished with 12%, 8%, and 4% of DAPOC.



Table 1 Vertical flammability test of untreated and treated cotton fabric

Samples	After-flame time (s)	After-glow time (s)	Char length (mm)	Smoldering cigarette test before washing (minutes)	Smoldering cigarette test after washing (minutes)
Control fabric	10	25	0	0	0
4%	0	0	85	30	24
8%	0	0	67	32	27
12%	0	0	48	35	30

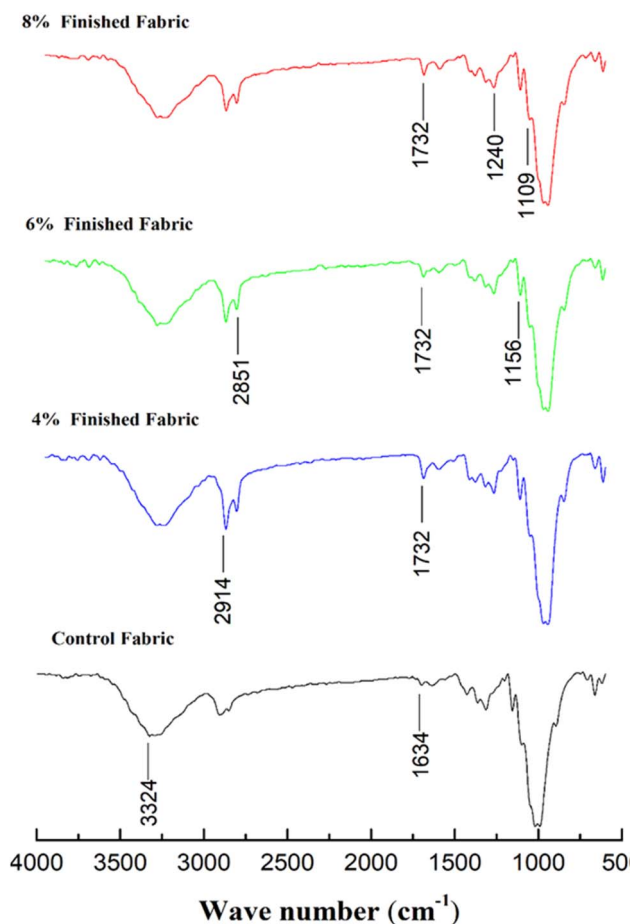


Fig. 6 FTIR spectrum of control fabric and fabric coated with 4%, 8%, and 12% mass concentrations of DAPOC.

2851  $\text{cm}^{-1}$  were linked with the stretching vibrations of C–H bonds in the extended carbon chain attached to the cotton substrate.<sup>59</sup> The spectrum peak at 1634  $\text{cm}^{-1}$  was identified as the vibration of C–O bonds in the untreated cotton fabric as depicted in Fig. 6.

The confirmation of the presence of the coating on the cotton fabrics was established through the observation of peaks at 1732 and 1240  $\text{cm}^{-1}$ . These peaks can be attributed to the stretching vibrations of C=O groups and P=O groups, respectively.<sup>60</sup> The peaks identified at 1109  $\text{cm}^{-1}$  in both the untreated and treated sample spectra were linked with the existence of C–O–C bonds within the cellulose structure.<sup>61</sup> These findings indicate that the newly developed finish was successfully grafted to the cellulose substrate by ester bond formation.

### X-ray diffraction (XRD)

The study involved an analysis of spectrum band intensities and the assessment of crystalline and amorphous region areas, as depicted in Fig. 7. The peak broadening at 15.1° and 16.7°  $2\theta$  reflection was attributed to the crystallographic plane (1–10) and (110), respectively, while the peak broadening at 22.8° and 34.2°  $2\theta$  reflection was associated with the crystallographic plane (200) and (004) respectively.<sup>46</sup>

The intensity of the diffraction peaks in the finished cotton fibers was almost identical to that of the pristine sample. Because the newly developed finish is hydrophobic, it faced difficulties penetrating the cotton fibers' inner polar space. As a result, the crystal structure of the original cotton fiber remained largely unaltered during the finishing process, showing that the DAPOC was predominantly attached to the outermost surface of cotton fibers.

### Thermogravimetric analysis (TGA)

Thermal analyses of the cotton fabric samples were carried out by using thermogravimetric analysis in a nitrogen environment as shown in Fig. 8. The untreated control and cotton fabrics treated with 12% of finish exhibited three distinct phases of weight reduction. Below 100 °C, the decrease in weight was ascribed to the dehydration process. The initial decomposition temperature at which the control sample experienced a 5% weight loss, was measured at 279 °C.

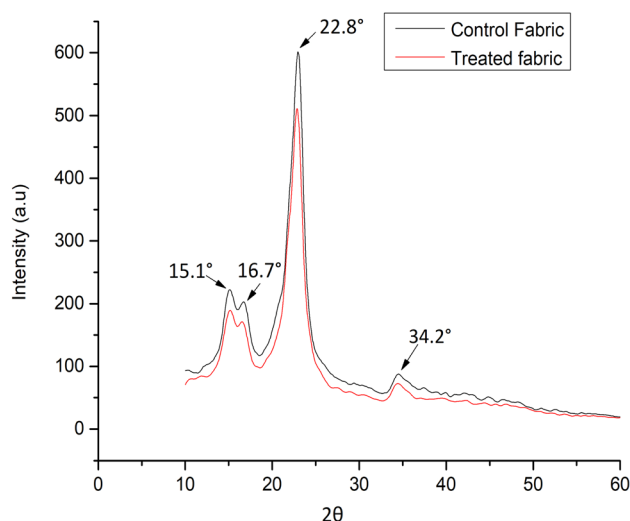


Fig. 7 XRD spectrum of control sample and finished fabric.



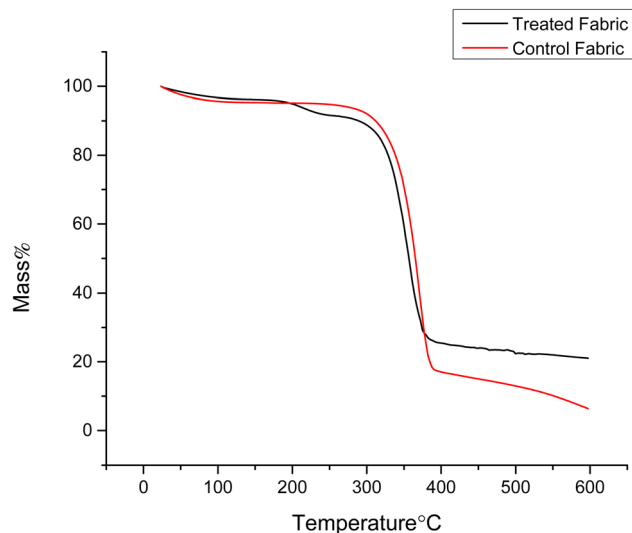


Fig. 8 Thermogravimetric analysis curves of the pristine and treated cotton samples under a  $N_2$  atmosphere.

The pristine cotton experienced significant thermal decomposition, primarily within the temperature range of 318.7 to 390.5 °C, resulting in a residue of 25.5%. During the third stage of thermal decomposition (390.7–600.1 °C), the rate of weight loss for untreated cotton fabrics decreased. At 600.1 °C, only 5.2% of the initial mass remained. The treated cotton fabric experienced significant thermal decomposition primarily within the 306.9 to 382.7 °C, resulting in a residue of 32.5%. During the third stage of thermal decomposition (382.7–595.2 °C),

the rate of weight loss for finished cotton fabric decreased. At 595.2 °C, only 16.2% of the initial mass remained. The treated cotton exhibited a significant decrease in decomposition. This was attributed to the presence of phosphorus components in the finishing agents. These components transformed into phosphoric acid during combustion. Phosphoric acid is known for its effective dehydration properties, which expedited the processes of cellulose dehydration and carbonization.<sup>45</sup>

#### Energy-dispersive X-ray spectroscopy (EDX)

EDX spectrum of the control cotton and cotton sample treated with a newly developed recipe is shown in Fig. 9. The treated cotton fabrics exhibited a distribution of carbon (C), oxygen (O), and phosphorus (P) elements. Notably, carbon, oxygen, and phosphorus displayed distinct peaks at energy levels of 0.27 keV, 0.5 keV, and 2 keV, respectively. The mass percentage concentrations of C and O on the treated sample exceeded those on the untreated sample, attributable to the extended carbon chain present in the stearic acid. This observation provides evidence that the newly developed finish successfully adhered to the cotton fibers. In contrast, these extended chains do not incorporate harmful formaldehyde and fluorine elements, unlike the flame retardants and water repellents commonly found in commercial products.

#### Morphological analysis

The surface morphologies of various samples have been shown in Fig. 10. The control sample (10a), the sample treated with

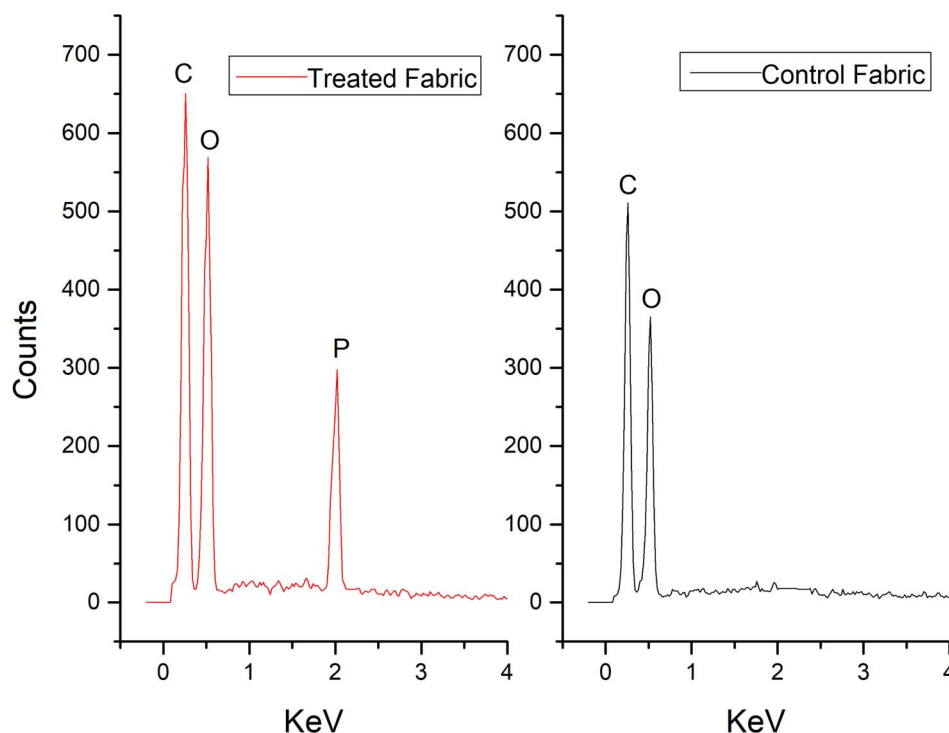


Fig. 9 Energy-dispersive X-ray spectra: (a) treated fabric, (b) control Fabric.



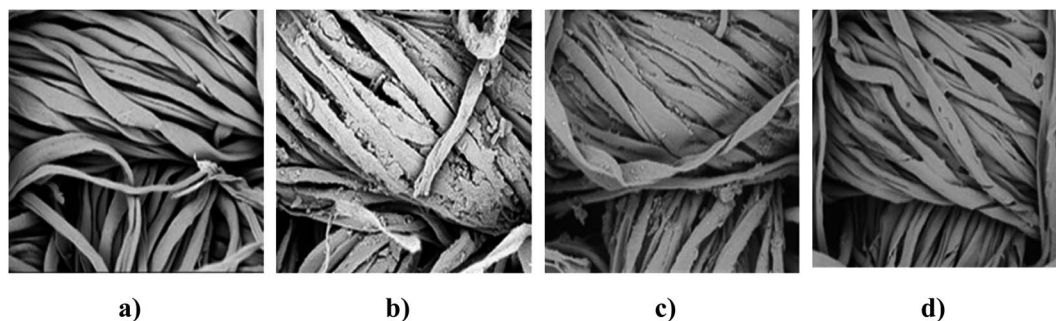


Fig. 10 SEM images of (a) control sample, (b) 12% treated sample prior to washing, (c) 12% finished sample followed by 20 wash cycles, (d) burnt treated sample.

12% newly developed recipe (10b), the 12% newly developed recipe-treated sample after undergoing 20 laundering cycles (10c), and the char residue of the finished sample (10d).

Compared to the control sample, which exhibited notably smooth surfaces with a wavy structure, the treated sample displayed a rougher surface texture.<sup>62</sup> The increased roughness is expected to enhance the hydrophobic properties of cotton fabrics by reducing surface energy. This can be attributed to the hydrophobic characteristics of the newly developed finish, characterized by its long hydrocarbon chain. Due to this property, the molecule encounters difficulty penetrating the inner spaces of cotton fibers. Even following 20 laundering cycles, the upper surface of the cotton fibers retained a slight roughness. The burnt cotton fibers managed to preserve their microstructure, and the resulting carbon residue maintained the original shape of the cotton fibers prior to combustion.

### Durability of DAPOC

The study evaluates the washing durability of samples to determine if the water repellency of cotton textiles with flame-retardant features could maintain their functionality over a prolonged period. The testing procedure adhered to the AATCC 61-2006 standard, a recognized method for evaluating the colorfastness and durability of textiles after laundering.

Fig. 11 presents the water contact angles of cotton treated with finishing agents at mass concentrations of 4%, 8%, and 12% after 20 laundering cycles (LCs). The cotton fabrics finished with 4%, 8%, and 12% newly developed recipes displayed respective contact angles of 138°, 145°, and 148.5°, respectively, after 20 LCs. In comparison to the pristine cotton fabrics, the treated ones sustained significantly higher contact angles, demonstrating remarkable water repellent properties even after multiple washes. Consequently, the finished cotton fabrics efficiently ensured the longevity of their hydrophobic characteristics through laundering.

Table 2 presents the results of the vertical flame test for the pristine cotton fabrics and those treated with finishing agents. At concentrations of 4%, 8%, and 12% after undergoing 20 laundering cycles (LCs), the decrease in char length was 75 mm, 56 mm, and 40 mm respectively. For the control cotton fabrics, the after-flame time was 7 seconds, while the after-glow time was 8 seconds. On the other hand, the cotton fabrics treated

with finishing agents with 4%, 8%, and 12% exhibited reduced after-flame times of 7 seconds, 6 seconds, and 5 seconds, respectively. Notably, all treated fabrics showed an after-glow time of 0 seconds. Following washing, the flame-retardant properties of the treated cotton fabric exhibited a slight reduction compared to the unwashed treated cotton.

### Antimicrobial resistance of the finished cotton fabric

As expected, the control cotton fabric showed no antibacterial efficacy against either *E. coli* or *S. aureus*, given cotton's susceptibility to microbial activity. Notably, citric acid

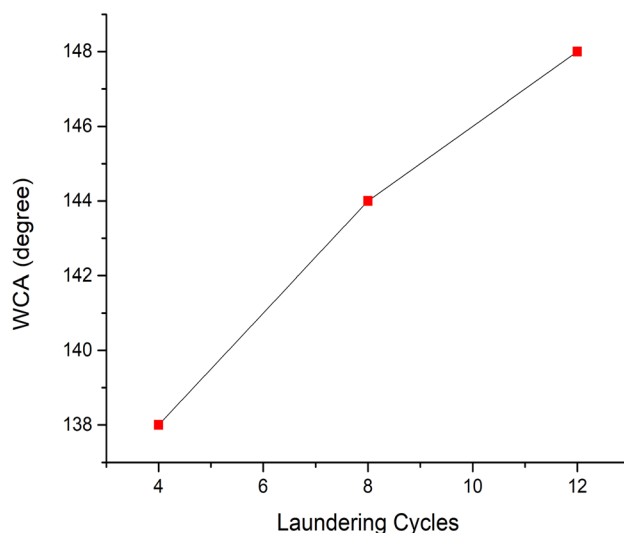


Fig. 11 Water contact angle of 4%, 8%, and 12% mass concentration samples after 20 LCs.

Table 2 Vertical flame test of control and finished samples after 20 LCs

Samples	After-flame time (s)	After-glow time (s)	Char length (mm)
Control fabric	9	10	0
4%	7	0	75
8%	6	0	56
12%	5	0	40



Table 3 Inhibition zone for untreated and treated cotton fabric

Samples	Zone of inhibition (mm)	
	<i>E. coli</i>	<i>S. aureus</i>
Control fabric	0	0
4%	0.19	0.18
8%	0.21	0.15
12%	0.26	0.12

demonstrated strong antibacterial properties.<sup>63</sup> The treated cotton fabric with a 12% mass concentration displayed a larger inhibition zone than those treated with 4% and 8% mass concentrations. Specifically, for *Escherichia coli*, the inhibition zones were 0.26 mm, 0.21 mm, and 0.19 mm for 12%, 8%, and 4% mass concentrations of the finishing agent, respectively, as shown in Table 3. Meanwhile, the inhibition zones for *Staphylococcus aureus* were 0.18 mm, 0.15 mm, and 0.12 mm for 12%, 8%, and 4% mass concentrations of the finishing agent, respectively.

## Conclusions

A novel fluorine-free finishing agent with hydrophobic and flame-retardant properties was synthesized and applied to cotton fabric. When applied to cotton fabrics, it endowed them with hydrophobicity and flame retardancy. The treated cotton fabrics' water contact angle (WCA) was 151.9°, signifying that the finishing agent rendered the cotton fabrics super-hydrophobic. Impressively, even after 20 laundering cycles (LCs), the contact angle remained steady at 148.5°. In the vertical flame burning test, it was observed that the finished cotton fabrics demonstrated an increased Limiting Oxygen Index (LOI) value of 27.0%. Even after undergoing 20 wash cycles, this value remained elevated at 26.4%, surpassing the original LOI of 18% for pristine cotton. Furthermore, the char length for the treated cotton fabric was 48 mm, which persisted at 40 mm even after 20 wash cycles. Moreover, findings from the TGA test indicated that the finished cotton fabrics exhibited flame-retardant properties. The FTIR and EDX analyses confirmed the successful covalent bonding of the finishing agent to the cotton fibers. As a result, the cotton fabrics exhibited long-lasting hydrophobic and flame-retardant properties. The treated cotton fabric also exhibits a significant zone of inhibition for both *Escherichia coli* and *Staphylococcus aureus*, as citric acid exhibits good antimicrobial properties. Additionally, XRD and SEM revealed minimal alterations in the surface morphology of the finished cotton fabrics. In summary, this novel finishing agent DAPOC, offers a sustainable and eco-friendly solution for rendering cotton fabrics both durable and hydrophobic while providing flame-retardant and antimicrobial properties.

## Conflicts of interest

No conflicts of interest exist that need to be disclosed.

## Acknowledgements

The authors are cordially grateful to the University of Engineering and Technology, Lahore for supporting this work [ORIC/100-ASRB/1990].

## References

- 1 R. Paul, *High Performance Technical Textiles*, John Wiley & Sons, 2019.
- 2 T. A. Khattab, M. Rehan and T. Hamouda, *Carbohydr. Polym.*, 2018, **195**, 143–152.
- 3 M. Rehan, T. A. Khattab, A. Barohum, L. Gätjen and R. Wilken, *Carbohydr. Polym.*, 2018, **197**, 227–236.
- 4 T. A. Khattab, M. Rehan, Y. Hamdy and T. I. Shaheen, *Ind. Eng. Chem. Res.*, 2018, **57**, 11483–11492.
- 5 X.-H. Shi, Q.-Y. Liu, X.-L. Li, A.-K. Du, J.-W. Niu, Y.-M. Li, Z. Li, M. Wang and D.-Y. Wang, *Polym. Degrad. Stab.*, 2022, **197**, 109839.
- 6 C. Liao, Y. Li, M. Gao, Y. Xia, W. Chai, X. Su, Z. Zheng and Y. Liu, *Colloids Surf., A*, 2022, **651**, 129647.
- 7 F. Gao, Y. Mi, X. Wu, J. Yao, Q. Qi, W. Chen and Z. Cao, *Carbohydr. Polym.*, 2022, **278**, 118935.
- 8 R. Sharif, M. Mohsin, N. Ramzan, S. W. Ahmad and H. G. Qutab, *J. Nat. Fibers*, 2022, **19**, 1632–1647.
- 9 I. S. Tania, M. Ali and M. Akter, *J. Eng. Fibers Fabr.*, 2022, **17**, 15589250221136378.
- 10 Y. Liu, D. Ding, Y. Lu, Y. Chen, Y. Liao, G. Zhang and F. Zhang, *Colloids Surf., A*, 2022, 129005.
- 11 X. Liu, Q. Shao, J. Cao, Z. Du and W. Yu, *Cellulose*, 2022, **1**–14.
- 12 C. Dong, Z. Lu, F. Zhang, P. Zhu, P. Wang, Y. Che and S. Sui, *J. Therm. Anal. Calorim.*, 2016, **123**, 535–544.
- 13 Z. Fei, B. Liu, M. Zhu, W. Wang and D. Yu, *Cellulose*, 2018, **25**, 3179–3188.
- 14 A. Berendjchi, R. Khajavi and M. E. Yazdanshenas, *Nanoscale Res. Lett.*, 2011, **6**, 1–8.
- 15 G. Pan, X. Xiao and Z. Ye, *Surf. Coat. Technol.*, 2019, **360**, 318–328.
- 16 M. Y. Soliman and A. G. Hassabo, *J. Text. Color. Polym. Sci.*, 2021, **18**, 97–110.
- 17 R. Shen, T. Fan, Y. Quan, R. Ma, Z. Zhang, Y. Li and Q. Wang, *Mater. Chem. Phys.*, 2022, **282**, 125986.
- 18 X. Chen, F. Fang, X. Zhang, X. Ding, Y. Wang, L. Chen and X. Tian, *RSC Adv.*, 2016, **6**, 27669–27676.
- 19 N. Onar and G. Mete, *J. Text. Inst.*, 2016, **107**, 1463–1477.
- 20 L. Liu, Z. Huang, Y. Pan, X. Wang, L. Song and Y. Hu, *Cellulose*, 2018, **25**, 4791–4803.
- 21 R. Sharif, M. Mohsin, S. Sardar, N. Ramzan and Z. A. Raza, *J. Nat. Fibers*, 2022, **19**, 12473–12485.
- 22 H. G. Qutab, M. Mohsin, N. Ramzan, S. W. Ahmad and S. Sardar, *J. Nat. Fibers*, 2021, **18**, 1913–1923.
- 23 D. Sun, W. Wang and D. Yu, *Cellulose*, 2017, **24**, 4519–4531.
- 24 H. Qin, X. Li, X. Zhang and Z. Guo, *New J. Chem.*, 2019, **43**, 5839–5848.
- 25 M.-J. Kim, I.-Y. Jeon, J.-M. Seo, L. Dai and J.-B. Baek, *ACS Nano*, 2014, **8**, 2820–2825.



- 26 M. Maturi, C. Spanu, N. Fernández-Delgado, S. I. Molina, M. Comes Franchini, E. Locatelli and A. Sanz de León, *Addit. Manuf.*, 2023, **61**, 103342.
- 27 M. Salajková, L. A. Berglund and Q. Zhou, *J. Mater. Chem.*, 2012, **22**, 19798–19805.
- 28 P. Chauhan, A. Kumar and B. Bhushan, *J. Colloid Interface Sci.*, 2019, **535**, 66–74.
- 29 C. Wei, Y. Tang, G. Zhang, Q. Zhang, X. Zhan and F. Chen, *RSC Adv.*, 2016, **6**, 74340–74348.
- 30 R. Sharif, M. Mohsin, H. G. Qutab, F. Saleem, S. Bano, R. Nasir and A. Wahlah, *Chem. Pap.*, 2023, **77**, 3547–3560.
- 31 M. Zahid, J. A. Heredia-Guerrero, A. Athanassiou and I. S. Bayer, *Chem. Eng. J.*, 2017, **319**, 321–332.
- 32 H. Lei, M. Xiong, J. Xiao, L. Zheng, Y. Zhu, X. Li, Q. Zhuang and Z. Han, *Prog. Org. Coat.*, 2017, **103**, 182–192.
- 33 P. Grandjean, E. W. Andersen, E. Budtz-Jørgensen, F. Nielsen, K. Mølbak, P. Weihe and C. Heilmann, *Jama*, 2012, **307**, 391–397.
- 34 C. Fei, J. K. McLaughlin, L. Lipworth and J. Olsen, *Hum. Reprod.*, 2009, **24**, 1200–1205.
- 35 S. Tragoonwichian, P. Kothary, A. Siriviriyannun, A. Edgar and N. Yanumet, *Colloids Surf., A*, 2011, **384**, 381–387.
- 36 R. Sharif, M. Mohsin, N. Ramzan, S. Sardar, S. W. Ahmad and W. Ahtisham, *J. Nat. Fibers*, 2022, **19**, 5637–5650.
- 37 S. Perera, B. Bhushan, R. Bandara, G. Rajapakse, S. Rajapakse and C. Bandara, *Colloids Surf., A*, 2013, **436**, 975–989.
- 38 H. Holmquist, S. Schellenberger, I. van Der Veen, G. Peters, P. Leonards and I. T. Cousins, *Environ. Int.*, 2016, **91**, 251–264.
- 39 T. A. Dankovich and Y.-L. Hsieh, *Cellulose*, 2007, **14**, 469–480.
- 40 Z. Huang, R. S. Gurney, T. Wang and D. Liu, *J. Colloid Interface Sci.*, 2018, **527**, 107–116.
- 41 M. Mohsin, C. Carr and M. Rigout, *Fibers Polym.*, 2013, **14**, 724–728.
- 42 M. Mohsin, N. Sarwar, S. Ahmad, A. Rasheed, F. Ahmad, A. Afzal and S. Zafar, *J. Cleaner Prod.*, 2016, **112**, 3525–3530.
- 43 H. G. Qutab, M. Mohsin, N. Ramzan, S. W. Ahmad and S. Sardar, *Cellul. Chem. Technol.*, 2019, **54**, 135–148.
- 44 Z.-F. Li, C.-J. Zhang, L. Cui, P. Zhu, C. Yan and Y. Liu, *J. Anal. Appl. Pyrolysis*, 2017, **123**, 216–223.
- 45 S. Li, S. Huang, F. Xu, T. Zhao, F. Zhang and G. Zhang, *Cellulose*, 2020, **27**, 3989–4005.
- 46 Y. Jia, Y. Hu, D. Zheng, G. Zhang, F. Zhang and Y. Liang, *Cellulose*, 2017, **24**, 1159–1170.
- 47 F. Zhang, W. Gao, Y. Jia, Y. Lu and G. Zhang, *Carbohydr. Polym.*, 2018, **199**, 256–265.
- 48 Y. Feng, Y. Zhou, D. Li, S. He, F. Zhang and G. Zhang, *Carbohydr. Polym.*, 2017, **175**, 636–644.
- 49 J. Jing, Y. Zhang, Z.-P. Fang and D.-Y. Wang, *Compos. Sci. Technol.*, 2018, **165**, 161–167.
- 50 Y. Qian, S. Zhou and X. Chen, *J. Thermoplast. Compos. Mater.*, 2018, **31**, 1295–1309.
- 51 H. Pan, W. Wang, Y. Pan, W. Zeng, J. Zhan, L. Song, Y. Hu and K. M. Liew, *Cellulose*, 2015, **22**, 911–923.
- 52 T. Suryaprabha and M. G. Sethuraman, *Cellulose*, 2018, **25**, 3151–3161.
- 53 D. Zhang, B. L. Williams, S. B. Shrestha, Z. Nasir, E. M. Becher, B. J. Lofink, V. H. Santos, H. Patel, X. Peng and L. Sun, *J. Colloid Interface Sci.*, 2017, **505**, 892–899.
- 54 D. Lin, X. Zeng, H. Li, X. Lai and T. Wu, *J. Colloid Interface Sci.*, 2019, **533**, 198–206.
- 55 A. Sarı, A. Biçer and A. Karaipekli, *Mater. Lett.*, 2009, **63**, 1213–1216.
- 56 V. Costa and R. Simoes, *J. Mater. Sci.*, 2022, **57**, 11443–11459.
- 57 C. Ling, L. Guo and Z. Wang, *Ind. Crops Prod.*, 2023, **194**, 116264.
- 58 G. Rosace, C. Colleoni, V. Trovato, G. Iacono and G. Malucelli, *Cellulose*, 2017, **24**, 3095–3108.
- 59 P. Dumas and L. Miller, *Vib. Spectrosc.*, 2003, **32**, 3–21.
- 60 H. A. Cheema, A. El-Shafei and P. J. Hauser, *Carbohydr. Polym.*, 2013, **92**, 885–893.
- 61 W.-W. Gao, G.-X. Zhang and F.-X. Zhang, *Cellulose*, 2015, **22**, 2787–2796.
- 62 P. Li, B. Wang, Y.-J. Xu, Z. Jiang, C. Dong, Y. Liu and P. Zhu, *ACS Sustain. Chem. Eng.*, 2019, **7**, 19246–19256.
- 63 I. Bramhecha and J. Sheikh, *Ind. Eng. Chem. Res.*, 2019, **58**, 21252–21261.

